

Light-scattering cross sections of Ca^{2+} and the calcium-cation-vacancy complex in KBr

W. J. Fredericks and Paul R. Collins*

Chemistry Department, Oregon State University, Corvallis, Oregon 97331

David F. Edwards†

Los Alamos National Laboratory, Los Alamos, New Mexico 87545

(Received 20 October 1986)

Measurements of a scattering ratio η_T as a function of total calcium concentration were used to estimate the scattering cross section σ of Ca^{2+} and the calcium-cation-vacancy complex as impurities in KBr. As theory predicts, no difference in σ for these species was detected. The experimental σ for these species was $5.9 \times 10^{-26} \text{ cm}^2$, about an order of magnitude larger than the theoretical value.

Mill's¹ calculation of the scattering cross section of homovalent impurities in alkali halides extended Rayleigh theory to include scattering from the strain halo due to the elastic displacement of the ions adjacent to the impurity. Arora *et al.*² added scattering from the Coulomb halo produced by the Coulomb strain field around aliovalent impurities. Although much work has been reported on impurity scattering in alkali halides,³ no cross-section measurements have been made. Three problems hamper cross-section measurements: An inability to accurately compare absolute scattering intensities from different crystal samples, difficulty in producing crystals with a single impurity species, and inhomogeneity of the impurity distribution within the crystal.

In this work the ratio of the intensity of the unshifted band,⁴ I_G , to that of the Mandel'shtam-Brillouin (MB) bands, $I_G/2I_{\text{MB}}$, was measured at various impurity concentrations. If the crystals are pure and perfect this ratio is the Landau-Placzek ratio, η_{LP} . In real crystals this ratio, η_T , is usually larger than its theoretical value.⁵ The experimental value of the ratio can be expressed as

$\eta_T = \eta_{\text{LP}} + \sum \eta_i$, where η_i are the ratios due to excess scattering from impurities and imperfections. Figure 1 shows the effect of impurities and their state of aggregation on η_T . The increase in scattering from aggregation of impurities is very large. At room temperature the intensity of the MB bands is not affected by impurity scattering. This is illustrated in Fig. 2. Note that the MB intensities are not affected by either the impurity concentration or its state of aggregation. The small variations are due to differences in laser power and to a lesser extent to changes in operation of the Fabry-Perot interferometer. The apparatus used for these measurements is based on a Burleigh Fabry-Perot interferometer DAS-1 and Spectra Physics Model 165-08 argon laser; it is described elsewhere.⁵ The advantage of using this ratio is that it is independent of variations of experimental conditions because the intensity of the MB bands provides an internal standard which corrects for these variations among measurements.

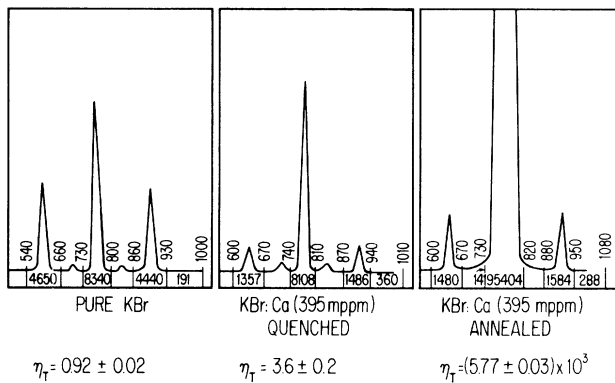


FIG. 1. Scattering spectra for pure, impure quenched, and impure annealed KBr crystals. The noise was removed when spectra copied.

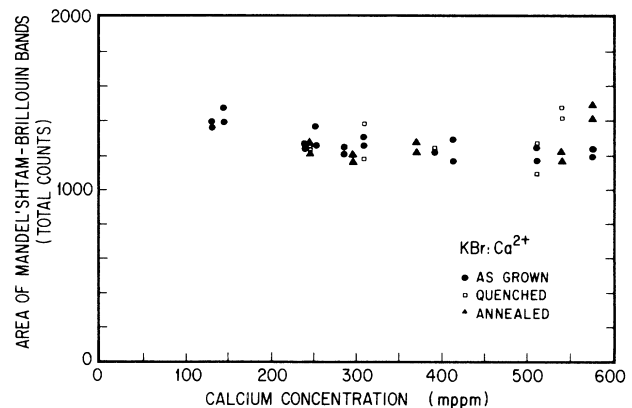


FIG. 2. The intensity of the MB bands in quenched, as grown, and annealed KBr crystals with various calcium concentrations. The variations are due to changes in laser power and experimental parameters. There is no concentration dependence observable.

TABLE I. Characteristics of calcium in KBr. $\text{Ca}V_c$ denotes a calcium-cation-vacancy complex, and V_a denotes an anion vacancy complex.

	Radii (Å)					
	Pauling ^a	Shannon ^b			Polarizability, α , (cm ³)	
K^+	1.33	1.37			1.14 ^c	
Ca^{2+}	0.99	1.00			1.14 ^d	
Br^-	1.95	1.96			4.28 ^e	
Solubility as maximum free Ca^{2+} concentration (mole fraction, χ)						
T (°C)	550	450	350	250	150	25
χ (10^4)	5.7	2.8	1.1	0.31	0.005	0.0007
Defect Concentrations χ (10^{-4})						
Total	CaCa^{2+}	550°C			450°C	
		$\text{Ca}V_c^+$	V_a^+	Ca^{2+}	$\text{Ca}V_c^+$	V_a^+
5.45	2.16	3.29	$4.42(10^{-4})$	1.34	4.11	$5.13(10^{-6})$
2.48	1.30	4.11	$7.35(10^{-4})$	0.84	1.63	$8.15(10^{-6})$

^aReference 8.

^bReference 9.

^cReference 10.

^dReference 11.

Any alkali halide containing a divalent cationic impurity, M , will contain at least two impurity species, M^{2+} and a metal-cation-vacancy complex (MV_c^+). The solubility⁶ of calcium and the fraction⁷ of impurity and intrinsic defects are given in Table I. If a calcium-containing crystal is slowly cooled the impurity precipitates. To prevent diffusion of the impurities into clusters the crystals must be cooled quickly from a temperature at which the solubility is not exceeded. Even then the impurity is present as a mixture of isolated calcium ions and impurity-vacancy complexes. (We will denote a cation-vacancy with V_c , and an anion vacancy with V_a .) The fraction associated as complexes depends on the total Ca^{2+} concentration and temperature. Calcium is an unusual impurity in KBr because its polarizability α_i is identical to that of K^+ , the ion for which it substitutes. Arora *et al.* calculate $\Delta\epsilon$ from $V_p\Delta\epsilon_0 = 4\pi(\alpha_i - \alpha_h)$, where i and h refer to impurity and host. Therefore $V_p\Delta\epsilon_0$ vanishes for Ca^{2+} and all scattering is due to the halos.

The divalent dopant was added as CaBr_2 made by dissolving Mallinckrodt standard luminescent (SL) grade CaCO_3 in aqueous HBr prepared by dissolving gaseous HBr in type-1 deionized water. The slightly acidic solution was evaporated to dryness in a Teflon dish in a Teflon-coated vacuum oven, then recrystallized from deionized water. After vacuum drying at 120°C it retained 3.7 mol of water of hydration as measured by calcium atomic emission analysis. This salt was added to Baker-analyzed KBr. KBr:Ca crystals were grown using the Czochralski method in a reactive-gas controlled-atmosphere puller.¹² The crystal growth parameters for each sample were as follows: Sample No. 1, 1934 mppm Ca^{2+} in melt, reactive-gas treatment started at 257°C with exchange sequence 9 HBr-3 Cl_2 -melt-3 HBr, crystal-pulled with flat-growth interface under dried argon at 1 cm/h and at 6 rpm rotation rate; sample No. 2, 893

ppm Ca^{2+} in melt, reactive-gas treatment started at 257°C with the exchange sequence 8 HBr-4 Cl_2 -melt-4 HBr, crystal-pulled with flat-growth interface under dried argon at same rate and rotation as for sample No. 1. Crystals approximately 9-cm long with about 3-cm wide {100} faces were grown. Based on Rolfe's¹³ absorption coefficient for OH^- in KBr at 214 nm the OH^- concentration in these crystals was less than 100 ppb.

The crystals were cleaved into sections 1-cm thick transverse to the pulling axis. Three cubes with approximately 1-cm (actually nine cubes are produced, only three used here) faces were cut from each section. The face closest to the seed was marked by beveling a corner. Atomic absorption analysis for calcium of the sections adjacent to the face nearest the seed and the face opposite to it gave the slight concentration gradient in each sample. From this and the distribution coefficient of calcium in KBr (Ref. 12) the concentration of calcium at any point in

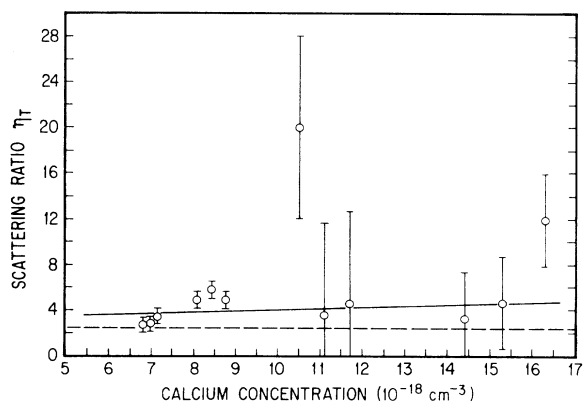


FIG. 3. The total scattering ratio, η_T , as a function of calcium concentration.

TABLE II. Theoretical scattering cross sections at 6328 Å².

	($\Delta\epsilon V_p$) (Å ³)	d	d_c	S	σ_0 (10 ²⁷ cm ²)	σ
KBr: V_c	-14.3	-0.14	-1.2	0.048	1.05	0.05
KBr: V_a	-53.8	-0.038	-0.31	0.51	14.9	7.7
KBr:Ca	0					1.9
KBr:Ca V_c	14.3	-0.36	0	1.77	1.1	1.9

the crystal could be estimated. Two cubes from each section were sealed in individual flat-bottomed, HBr-dried quartz tubes. Both were heated to 550°C; one set was annealed over 25 h to room temperature, the other quenched to 0°C in ice water. Test with thermocouples in a similar sample indicated the quench time to be about 20 s.

The Fabry-Perot interferometer was operated in the triple-pass mode. Typically the free spectral range (FRS) was 0.3905±0.004 Å. The finesse, measured as the ratio of FRS to the total apparatus half-width at half maximum was about 50. The geometry allowed only a 90° scattering angle. To minimize surface scattering the samples were immersed in bromobenzene ($n = 1.5602$) as an index-matching fluid.

The ratio, η_T , of quenched crystals as a function of concentration is shown in Fig. 3. Based on 46 measurements of nine crystals the expected background scattering for pure KBr crystals⁴ produced by the same growth methods is shown as a dashed line at $\eta_T = 2.48$. None of the samples showed any indication of precipitation. The two measurements with η_T of 12 and 20 were deleted from the data used to calculate linear regression fit to the remaining ten points. Such abnormally large values result from improper quenching or problems during crystal growth. The slope of the line is 1.09×10^{-19} and the intercept 2.94, slightly larger than the 2.48 expected.

The impurity scattering coefficient, β_G , is given by

$$\beta_G = \sum_i \sigma_i N_i, \quad (1)$$

where σ_i is the cross section and N_i is the number of impurity scattering centers per cm³. The total scattering ratio is given by

$$\eta_T = I_G / 2I_{MB} = \beta_G / 2\beta_{MB}. \quad (2)$$

The impurity scattering coefficient can be calculated from

$$\beta_G = 2\beta_{MB}\eta_T, \quad (3)$$

in which β_{MB} for KBr is given, for these experimental conditions, by

$$\beta_{MB} = \frac{\pi^2 n^8 k T}{\lambda^4} \left[\frac{2p_{12}^2}{c_{11} + c_{12} + 2c_{44}} + \frac{p_{44}^2}{2c_{44}} \right]. \quad (4)$$

For KBr at 4880 Å, $\beta_{MB} = 2.7 \times 10^{-7}$ when calculated using the elastooptic coefficients p_{ij} and elastic constants c_{ij} that best fit the ratio β_{zz}/β_{xx} .⁵ Thus, the experimental value of σ_G is 5.9×10^{-26} cm².

Arora *et al.*² calculate theoretical cross sections of impurities as

$$\sigma = \sigma_0 S, \quad \text{where } \sigma_0 = \omega^4 (\Delta\epsilon_0 V_p)^2 / 6\pi c^4 \quad (5)$$

and

$$S = (1 + d_c - 5d/8)^2 + 135d^2/64 \quad (6)$$

The contribution from the strain halo, d , was given as

$$d = \Delta_1 P_2 / r_0 \Delta\epsilon_0 \quad (7)$$

in which Δ_1 is the change in the radius of the scatterer, r_0 , due to lattice relaxation and P_2 is $-\epsilon^2(p_{11} - p_{12})$. The Coulomb halo was given by

$$d_c = 3P_1 a_0^2 \Delta_c \cos(\pi r_0^2 / a_0^2). \quad (8)$$

Here $P_1 = \epsilon_0^2(p_{11} + 2p_{12})/3$, and $\Delta_c \cos(\pi r_0^2 / a_0^2)$ is a function that alternates the sign of the Coulomb lattice relaxation. a_0 is the anion-cation distance in KBr. Arora *et al.* obtain the cross sections for defect species present in these crystals shown in Table II. For the complex species the two defects are averaged over the sum of the polarizability changes.

Converting the cross section of Arora *et al.* to 4880 Å gives 5.4×10^{-27} cm². The experimental cross section at 5.9×10^{-26} cm² and theoretical cross sections differ by about an order of magnitude. Considering the uncertainty in estimates of Δ_1 , $\Delta\epsilon$, and r_0 this is remarkably good agreement. Some small difference may be attributed to choice of differing values of Pockel's constants in their P_1 and P_2 and those used in our estimate of β_{MB} . The only defect with a larger cross section is V_a , but χ_{V_a} is suppressed by χ_{Ca} (see Table I) so its contribution to σ is nothing. If $\sigma(Ca^{2+})$ and $\sigma(CaV_c)$ differ it is not discernible in these experiments. Treating the experimental cross section as a Rayleigh cross section gives ($\Delta\epsilon V_p$) equal to 63.6 Å³.

If KBr:Ca forms next-nearest-neighbor complexes, CaBr V_c :{100}, rather than nearest-neighbor complexes, Ca V_c :{110}, their cross sections would be larger. No experimental evidence for their existence has been reported. The recent shell-model calculations of defect energies of Corish *et al.*¹⁴ suggest they may be present.

This work was supported in part by the United States Department of Energy under Contract No. DE-AT06-80ET 35078 and No. W7405-ENG-36.

*Present address: Union Carbide, Electronics Division, Washougal, WA 98671.

†Present address: Lawrence Livermore National Laboratory, Livermore, CA 94550.

¹D. Mills, *J. Appl. Phys.* **51**, 5864 (1980).

²A. K. Arora, R. Kesavamoorthy, and D. Sahoo, *J. Phys. C* **15**, 4591 (1982).

³For extensive references see: A. K. Arora, R. Kesavamoorthy, A. K. Sood, G. Venkataraman, R. Krishnaswamy, and D. Sahoo, *J. Phys. Chem. Solids* **45**, 69 (1984), and Ref. 4.

⁴A. T. Young, *Phys. Today* **35**, 42 (1982).

⁵W. J. Fredericks, P. R. Collins, and D. F. Edwards, *J. Phys. Chem. Solids* **45**, 471 (1984).

⁶J. Rolfe, *Can. J. Phys.* **42**, 2195 (1964).

⁷S. Chandra and J. Rolfe, *Can. J. Phys.* **49**, 2298 (1971).

⁸L. Pauling, *The Nature of the Chemical Bond*, 3rd. ed. (Cornell University Press, New York, 1960), p. 514.

⁹R. D. Shannon, *Acta Cryst. A* **32**, 751 (1976).

¹⁰J. Pirrenne and E. Kartheuser, *Physica* **30**, 2005 (1964).

¹¹J. Tesson, A. Kahn, and W. Shockley, *Phys. Rev.* **92**, 890 (1953).

¹²P. R. Collins and W. J. Fredericks, *J. Cryst. Growth* **71**, 739 (1984).

¹³J. Rolfe, *Can. J. Phys.* **41**, 1525 (1963).

¹⁴J. Corish, J. M. Quigley, P. W. M. Jacobs, and C. R. A. Catlow, *Philos. Mag. A* **44**, 13 (1981).